University of Dundee

Biotinylation of an acetylenic tricyclic bis(cyanoenone) lowers its potency as an NRF2 activator while creating a novel activity against BACH1

Moreno, Rita; Casares, Laura; Higgins, Maureen; Ali, Kevin X.; Honda, Tadashi; Wiel, Clotilde

Citation for published version (APA):
Moreno, R., Casares, L., Higgins, M., Ali, K. X., Honda, T., Wiel, C., Sayin, V. I., Dinkova-Kostova, A. T., & de la Vega, L. (2022). Biotinylation of an acetylenic tricyclic bis(cyanoenone) lowers its potency as an NRF2 activator while creating a novel activity against BACH1. *Free Radical Biology and Medicine*, *191*, 203-211. https://doi.org/10.1016/j.freeradbiomed.2022.08.041

Original Contribution

Biotinylation of an acetylenic tricyclic bis(cyanoenone) lowers its potency as an NRF2 activator while creating a novel activity against BACH1

Rita Moreno [a], Laura Casares [a], Maureen Higgins [a], Kevin X. Ali [b,c], Tadashi Honda [d], Clotilde Wiel [b,c], Volkan I. Sayin [b,c], Albena T. Dinkova-Kostova [a,e], Laureano de la Vega [a,*]

[a] *Jacqui Wood Cancer Centre, Division of Cellular Medicine, School of Medicine, University of Dundee, UK*
[b] *Institute of Clinical Sciences, Department of Surgery, Sahlgrenska Center for Cancer Research, University of Gothenburg, Gothenburg, Sweden*
[c] *Wallenberg Centre for Molecular and Translational Medicine, University of Gothenburg, Gothenburg, Sweden*
[d] *Department of Chemistry and Institute of Chemical Biology & Drug Discovery, Stony Brook University, Stony Brook, NY, 11794-3400, USA*
[e] *Department of Medicine and Pharmacology and Molecular Sciences, Johns Hopkins University School of Medicine, Baltimore, MD, USA*

A B S T R A C T

The transcription factor BACH1 regulates the expression of a variety of genes including genes involved in oxidative stress responses, inflammation, cell motility, cancer cell invasion and cancer metabolism. Based on this, BACH1 has become a promising therapeutic target in cancer (as anti-metastatic target) and also in chronic conditions linked to oxidative stress and inflammation, where BACH1 inhibitors share a therapeutic space with activators of transcription factor NRF2. However, while there is a growing number of NRF2 activators, there are only a few described BACH1 inhibitors/degraders. The synthetic acetylenic tricyclic bis(cyanoenone), (±)-(4bS,8aR,10aS)-10a-ethynyl-4b,8,8-trimethyl-3,7-dioxo-3.4b,7,8,8a,9,10, 10a-octahydrophenanthrene-2,6-dicarbonitrile, TBE31 is a potent activator of NRF2 without any BACH1 activity. Herein we found that biotinylation of TBE31 greatly reduces its potency as NRF2 activator (50-75-fold less active) while acquiring a novel activity as a BACH1 degrader (100-200-fold more active). We demonstrate that TBE56, the biotinylated TBE31, interacts and promotes the degradation of BACH1 via a mechanism involving the E3 ligase FBXO22. TBE56 is a potent and sustained BACH1 degrader (50-fold more potent than hemin) and accordingly a powerful *HMOX1* inducer. TBE56 degrades BACH1 in lung and breast cancer cells, impairing breast cancer cell migration and invasion in a BACH1-dependent manner, while TBE31 has no significant effect. Altogether, our study identifies that the biotinylation of TBE31 provides novel activities with potential therapeutic value, providing a rationale for further characterisation of this and related compounds.

1. Background

The transcription factor BACH1 (broad complex, tramtrack and bric à brac and cap'n'collar homology 1), has recently gained visibility as a potential therapeutic target against a variety of inflammatory and chronic conditions ranging from Huntington's [1] and Parkinson's disease [2], bone destructive diseases [3], non-alcoholic steatohepatitis [4], atherosclerosis [5], insulin resistance [6], coronary artery disease [7] to aging-related conditions [8]. This is mainly based on the role of BACH1 as a transcriptional repressor of antioxidant and anti-inflammatory genes. The best characterised BACH1 target gene is HMOX1 [9,10] encoding an inducible enzyme with potent antioxidant and anti-inflammatory properties which is induced by the transcription factor NRF2 and repressed by BACH1. BACH1 competes with NRF2 for binding to sequences termed antioxidant response elements (AREs) within promoter regions, and also binds to non-ARE regions in genes not regulated by NRF2. Although the validated BACH1 target genes differ based on the cell lines and the model studied [2,11–15], HMOX1 is invariably the (or one of the) most induced genes in response to BACH1 inhibition/depletion, validating its value as a robust BACH1 reporter. While NRF2 activators induce the expression of numerous cytoprotective genes, BACH1-targetting compounds activate only a limited subset of these genes and are extremely potent at inducing *HMOX1*.

In addition to its therapeutic potential in chronic diseases, BACH1 is an attractive target in cancer. BACH1 is overexpressed in various tumour types correlating with poor prognosis and recurrence [11–13,16,17].


BACH1 promotes cancer cell invasion (*in vitro*) [11,12,16–20] and metastasis (*in vivo*) [11,12,16,17] in various cancer models by inducing the expression of genes involved in migration/invasion (such as *MMP1* and *CXCR4*) and metabolism (such as *HK2*) and by reducing the expression of epithelial genes involved in the epithelial to mesenchymal transition (such as *CDH1* and *FOXA1*). Additionally, BACH1 also decreases glucose utilisation and transcription of genes encoding electron transport chain (ETC) proteins in triple negative breast cancer (TNBC) [13]. Thus, targeting BACH1 impairs tumour spread in preclinical models of lung, breast and pancreatic cancer and is synthetically lethal in combination with ETC inhibitors in TNBC, impairing primary tumour growth.

Despite the potential of BACH1 as a therapeutic target, there are only a few described compounds that target BACH1 [1,2,21–23], and of those, two (HPP-971 from VTV-Therapeutics and ML-0207/ASP8731 from Astellas-Pharma) are in clinical development. Most of these compounds work by inducing BACH1 nuclear export and its cytoplasmic degradation [24,25], although we recently described two novel BACH1-targetting compounds (CDDO-Me and CDDO-TFEA) [26] that cause a change in BACH1 sub-cellular localisation from nuclear to cytoplasmic (without degrading BACH1), and a corresponding upregulation of HMOX1, implying that the nuclear export of BACH1 (even without its degradation) is sufficient to impair its activity.

It is still unclear how some compounds target BACH1, although a recent report shows that the electrophilic compound dimethyl fumarate (DMF) can covalently modify BACH1 cysteines *in vitro* [2], which suggests that BACH1 might be targeted by electrophiles. However, in cells, the electrophilic NRF2 activators sulforaphane, CDDO and TBE31 do not affect the levels of BACH1 [1,26], implying that electrophilicity is not sufficient. On the other hand, the electrophilic moiety within CDDO-Me is important for its activity in targeting BACH1 [26], suggesting that although electrophilicity is not sufficient, it might be necessary for the activity of some of these BACH1-targeting compounds. Thus, we hypothesised that the modification of known electrophiles might lead to the identification of novel BACH1-targeting compounds with therapeutic potential in a variety of conditions.

Here we describe that biotinylation of the potent NRF2 activator TBE31, which itself does not affect BACH1, confers a novel activity as a potent BACH1 degrader. TBE56, a biotinylated derivative of TBE31 [27], is less potent as an NRF2 activator (50-75-fold less potent than
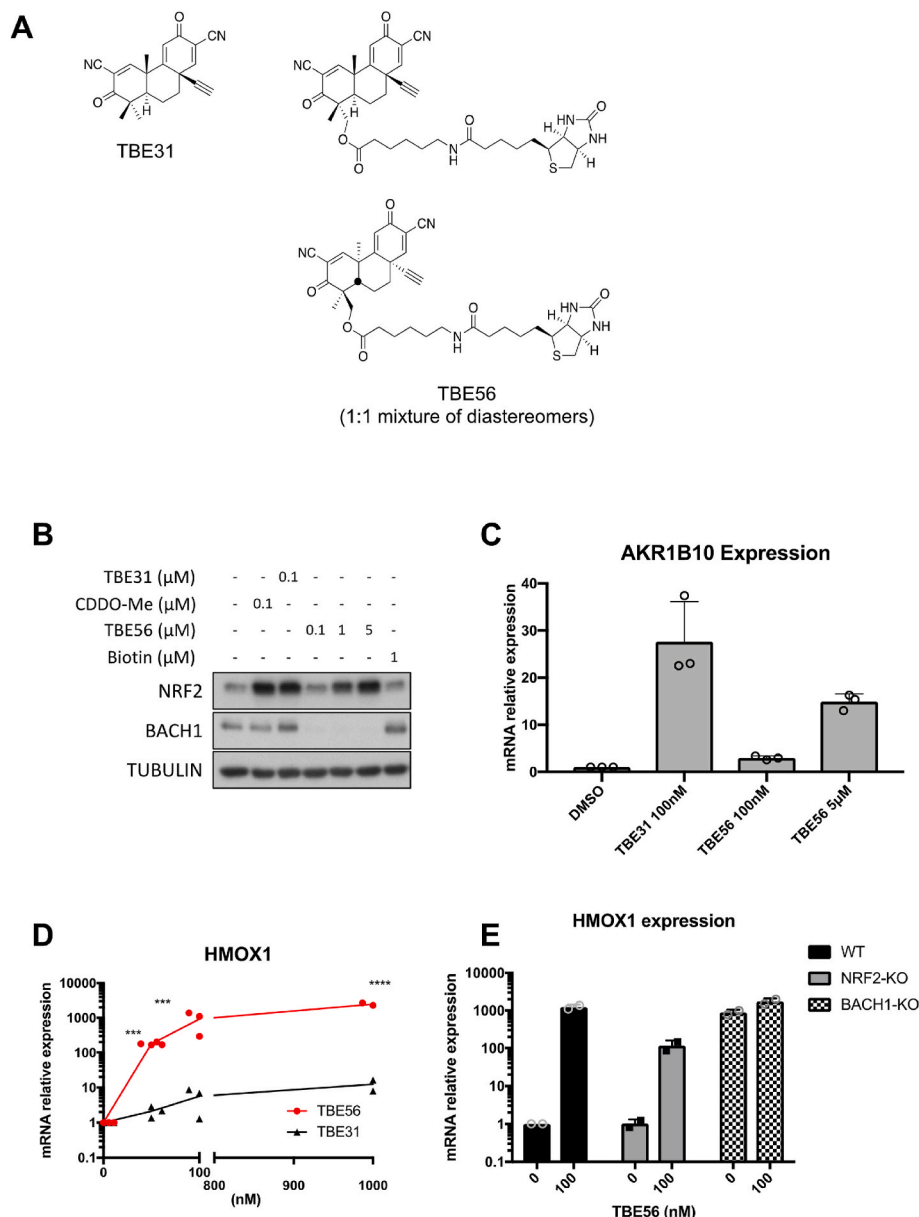
Fig. 1. **TBE56, but not TBE31, is a potent BACH1-targetting compound. A)** Structures of TBE31 and TBE56. **B)** HaCaT cells were treated with vehicle (DMSO, 0.1%, v/v) or with the indicated concentrations of either TBE31, CDDO-Me, TBE56 or biotin. After 3 h cells were lysed and samples were analysed by Western blot. **C)** HaCaT cells were treated with either DMSO (0.1%, v/v) or the indicated concentrations of TBE56 or TBE31. After 16 h cells were harvested and lysed and mRNA levels of *AKR1B10* were analysed by real-time qPCR. Data (n = 3) are expressed relative to the DMSO treated sample. **D)** HaCaT cells were treated with either DMSO (0.1%, v/v) or increasing concentrations of TBE56 or TBE31. After 16 h cells were harvested and lysed and mRNA levels of *HMOX1* were analysed by real-time qPCR. Data (n = 3) are expressed relative to the DMSO treated sample. ***P $\leq$ 0.001, ****P $\leq$ 0.0001. **E)** HaCaT WT, NRF2-KO or BACH1-KO cells were treated with either DMSO (0.1%, v/v) or with TBE56 (100 nM). After 16 h cells were harvested and lysed and mRNA levels of *HMOX1* were analysed by real-time qPCR as previously described. Data (n = 2) are expressed relative to the WT DMSO sample.

TBE31), but a potent BACH1 degrader in both non-malignant and cancer cell lines. Importantly, TBE56 but not TBE31, impairs cancer cell migration and invasion in a BACH1-dependent manner.

2. Results

2.1. TBE56, but not TBE31, is a potent BACH1-targeting compound

Compared to the tricyclic bis(cyanoenone) TBE31, its biotinylated derivative TBE56 (Fig. 1A) is a weak NRF2 activator (50-75-fold weaker, in agreement with a previous report [27]), with almost no effect at 100 nM, as assessed by NRF2 stabilisation and induction of its target gene AKR1B10 (Fig. 1B and C). In contrast, TBE56 is very potent in reducing the levels of BACH1, whereas TBE31 is completely inactive (Fig. 1B). Importantly, the effect of TBE56 on BACH1 is not due to biotin (Fig. 1A). We have previously shown that while in HaCaT cells AKR1B10 expression is an excellent reporter for NRF2 activation, HMOX1 induction is an excellent marker for BACH1 inhibition [1,21]. Compared with TBE31, TBE56 is a much more potent HMOX1 inducer (over 100 times more potent) (Fig. 1D). Moreover, similar to the BACH1-targeting compounds hemin and cannabidiol [1,21], the induction of HMOX1 in response to TBE56 still occurs in NRF2-KO cells, but not in BACH1-KO cells confirming the involvement of BACH1 (Fig. 1E). These data demonstrate that TBE56, but not TBE31, is a BACH1-targeting compound.

The best characterised BACH1-targeting compound is hemin, an oxidised form of heme. In HaCaT cells, TBE56 is > 50-fold more potent than hemin in reducing BACH1 levels (EC$_{50}$ = 44 nM for TBE56; EC$_{50}$ = 2.7 μM for hemin) (Fig. 2A and Suppl. Fig. S2A). In addition, compared

to vehicle-treatment, the levels of BACH1 were still ~80% lower 16 h post-treatment with TBE56, whereas they had largely recovered in hemin-treated cells, and further increased by TBE31 treatment (Fig. 2B). In all cell lines tested, 100 nM TBE56 was equally or more potent than 10 μM hemin at the 16-h timepoint (Suppl. Fig. S2B). The difference between the effect of TBE56 and hemin in potency and duration in decreasing the BACH1 levels is reflected at the induction of HMOX1 expression (Fig. 2C).

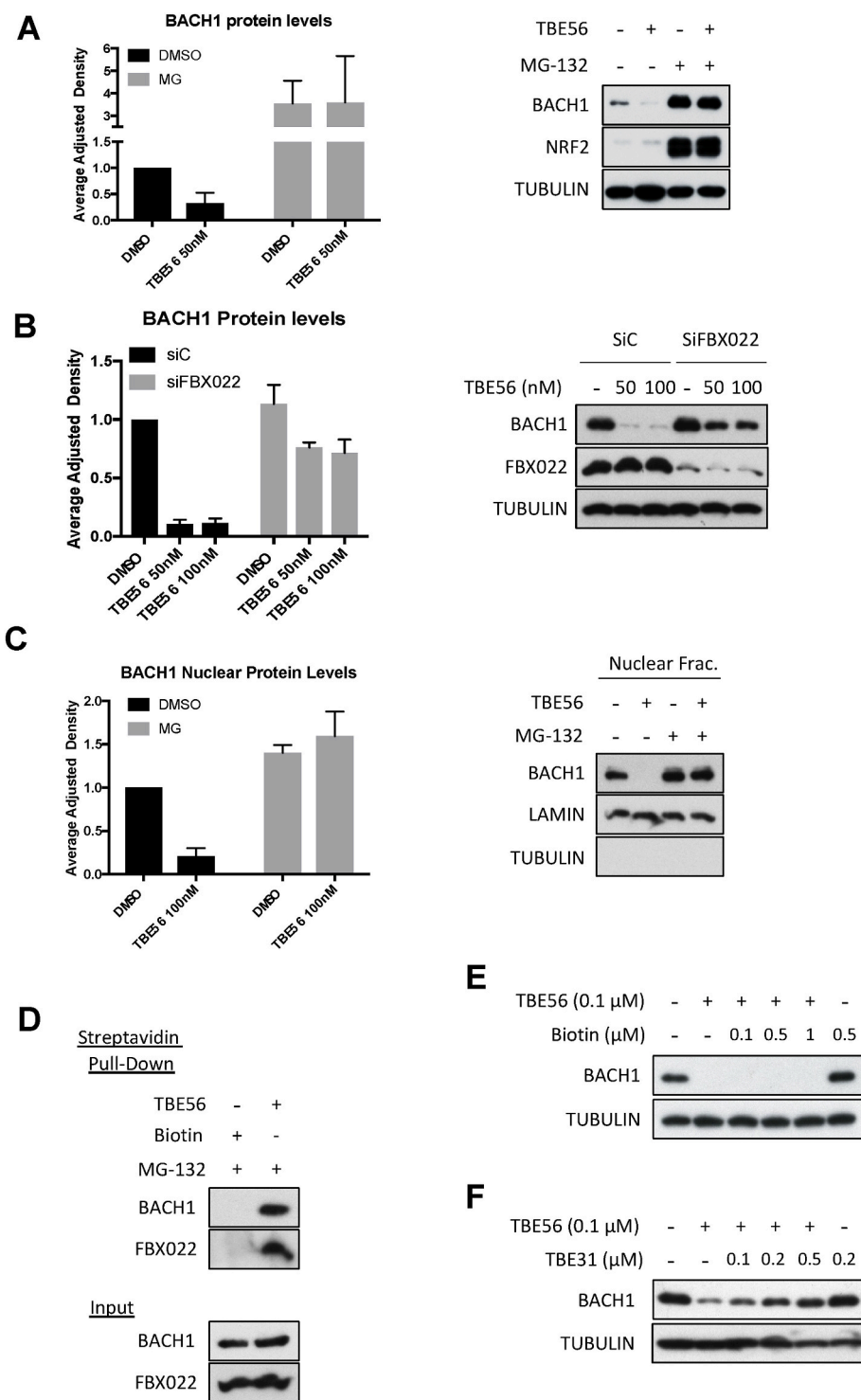### 2.2. TBE56 interacts with BACH1 and induces its degradation via FBXO22

To address the mechanism of action of TBE56, first we asked whether the reduction of BACH1 in response to TBE56 was due to BACH1 degradation. Pre-treatment with the proteasome inhibitor MG-132 impaired the decrease of BACH1 mediated by TBE56, suggesting that TBE56 induces BACH1 proteasomal degradation (Fig. 3A). A similar result was obtained using MLN4924 (Suppl. Fig. S3A), an inhibitor of the Nedd8-activating enzyme, which impairs the activity of Cullin-RING ligases (CRLs), the largest family of E3 ubiquitin ligases. As the CRL E3 ligase FBXO22 is a bona-fide BACH1 interactor [12], we tested whether FBXO22 was responsible for the BACH1 degradation mediated by TBE56. As shown in Fig. 3B, knockdown of FBXO22 impaired the effect of TBE56 on reducing the BACH1 levels, confirming the involvement of the E3 ligase in the degradation of BACH1 mediated by TBE56.

Interestingly, both MG-132 and MLN4924 recovered not only the total levels of BACH1, but also its nuclear levels (Fig. 3C and Suppl. Fig. S3B) in response to TBE56. This is in contrast with the effect that
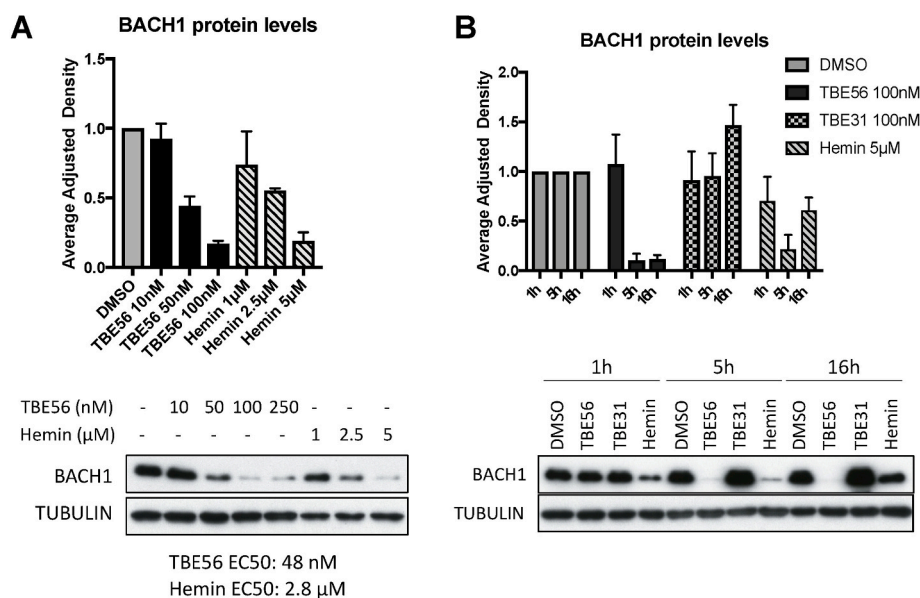
Fig. 2. The effect of TBE56 reducing BACH1 levels is more potent and sustained than that of Hemin. A) HaCaT cells were treated with vehicle (DMSO, 0.1%, v/v) or with increasing concentrations of either TBE56 or hemin. After 3 h cells were lysed, and samples were analysed by Western blot. Upper panel shows the quantification of BACH1 protein levels normalized for tubulin levels; lower panel is a representative blot. Data represent means ± SD (n = 3) and are expressed relative to the DMSO-treated samples. **B)** HaCaT cells were treated with DMSO (0.1%, v/v), TBE56 (100 nM), TBE31 (100 nM) or hemin (5 μM) for 1, 5 or 16 h. After that, cells were lysed and samples were analysed by Western blot. Upper panel shows the quantification of BACH1 protein levels normalized for tubulin levels; lower panel is a representative blot. Data represent means ± SD (n = 3) and are expressed relative to the DMSO-treated samples. **C)** HaCaT cells were treated with either DMSO (0.1%, v/v) TBE56 (100 nM) or hemin (5 μM) for 3, 6 or 16 h. After that, cells were harvested and lysed and mRNA levels of *HMOX1* were analysed by real-time qPCR. Data (n = 2–5) are expressed relative to the DMSO treated sample. **P ≤ 0.01.

Fig. 3. TBE56 interacts with BACH1 and induces its degradation via FBXO22. A) HaCaT cells were incubated with either DMSO (0.1%, v/v) or MG132 (10 μM) for 1 h. After that, either DMSO (−) or TBE56 (100 nM) was added. Three hours later, cells were harvested and samples were analysed by Western blot. Left panel shows the quantification of BACH1 protein levels normalized for tubulin levels; data represent means ± SD (n = 3) and are expressed relative to the DMSO-treated samples. Right panel is a representative blot. **B)** HaCaT cells transfected for 48 h with either siControl or siFBXO22 were treated with DMSO (0.1%, v/v) or TBE56 as indicated. Three hours later, cells were harvested and samples were analysed by Western blot. Left panel shows the quantification of BACH1 protein levels normalized for tubulin levels; data represent means ± SD (n = 4) and are expressed relative to the DMSO-treated samples. Right panel is a representative blot. **C)** HaCaT cells were incubated with either DMSO (0.1%, v/v) or MG132 (10 μM) for 1 h. After that, either DMSO (−) or TBE56 (100 nM) was added. Three hours later, cells were harvested and nuclear/cytoplasmic fractions were isolated and analysed for their levels of BACH1. Left panel shows the quantification of BACH1 nuclear protein levels normalized for LAMIN levels (n = 4); right panel is a representative blot. **D)** HaCaT cells were incubated with MG132 (10 μM) for 1 h. After that, either Biotin (100 nM) or TBE56 (100 nM) was added. Three hours later, cells were harvested, lysed and streptavidin beads were used to pull down biotin/TBE56. Input (5% of the sample before pull-down) and eluted fraction were analysed for the presence of BACH1. **E)** HaCaT cells were incubated with either DMSO (0.1%, v/v), TBE56 (100 nM) or biotin as indicated. Three hours later, cells were harvested, lysed and analysed for their levels of BACH1. **F)** As in E) but TBE31 was used instead of biotin.

proteasome inhibitors have on BACH1 nuclear levels when used with hemin (Suppl. Fig. S3C) or CBD [21], where the reduction of nuclear BACH1 is not impaired by MG-132. Hemin and CBD induce nuclear export and cytoplasmic degradation of BACH1 [21,25,28] and thus our results suggest that TBE56 has a different mechanism of action, most likely degrading BACH1 in the nucleus without a previous nuclear export step (although we cannot rule out other potential mechanisms). Furthermore, TBE56 promoted the degradation of a BACH1 mutant that is resistant to hemin (Suppl. Fig. S3D), further confirming the difference in the mechanisms of action between TBE56 and hemin.

To test whether TBE56 interacts with BACH1 we performed a pull down in the presence of MG-132 (Fig. 3D). We found that TBE56, but not free biotin, interacts with both BACH1 (which suggest a potential direct effect) and FBXO22. As free biotin does not interact with BACH1, we hypothesised that the TBE56-BACH1 interaction must be via its tricyclic TBE core group. To test this, we performed competition experiments against TBE56 with either increasing concentrations of free biotin or TBE31 and tested their effect on BACH1 levels. Free biotin did not impair the degradation of BACH1 mediated by TBE56 (Fig. 3E and Suppl. Fig. S3E), but TBE31 did (Fig. 3F and Suppl. Fig. S3F), further

suggesting that the interaction between TBE56 and BACH1 is via its tricyclic core group, and not via its biotin group.

2.3. TBE56 degrades BACH1 in a variety of cancer cells

Considering the relevance of BACH1 as a target in lung and breast cancer, next we performed a concentration- and time-dependent analysis of the ability of TBE56 to degrade BACH1 in four relevant cancer cell lines: two triple negative breast cancer cell lines (MDA-MB-231 and MDA-MB-468) and two lung cancer cell lines (A549 and H1299). As shown in Fig. 4A and Suppl. Fig. S4A, at the 5-h timepoint, TBE56 concentration-dependently promoted the degradation of BACH1 in all cell lines examined (being A549 the more resistant). Importantly, BACH1 degradation in response to TBE56 was still maintained at the 16-h timepoint (Fig. 4B and Suppl. Fig. S4B). Altogether, our results show that TBE56 is a potent and sustained BACH1 degrader.

Interestingly, after 16 h of treatment we observed a curious phenomenon: the degradation of BACH1 was maximal at the 100 nM TBE56 concentration, followed by either a plateau or even an increase in BACH1, reaching its highest levels at the 5 μM TBE56 concentration (this was not observed in A549 cells). While 5 μM of TBE56 might be outside

the range of useful concentrations in some cell lines (as indicated by the observed toxicity in MDA-MB-468 cells, Suppl. Fig. S4F) it was important to understand the dose response of the various cellular systems tested for selecting the correct concentration for the physiological readouts. Thus, we asked whether this accumulation of BACH1 was reflected on the expression of HMOX1. We reasoned that if the accumulated BACH1 in response to 5 μM TBE56 was active, the expression of HMOX1 would show a parallel opposite pattern, increasing in response to low concentrations of TBE56, and decreasing again with high concentrations. However, this was not observed. The expression of HMOX1 in all cell lines increased in a concentration-dependent manner (Fig. 4C), suggesting that either the observed accumulation of BACH1 was not functionally active, or BACH1 was outcompeted by another transcription factor, which was also affected by TBE56. In this context, we have previously shown that the BACH1-targetting compounds CDDO-Me and CDDO-TFEA induce BACH1 nuclear export and cytoplasmic accumulation, which induces HMOX1 expression without reducing the total BACH1 levels, demonstrating (as expected) that cytoplasmic BACH1 does not regulate HMOX1 expression. To test whether that was also the case for TBE56, we analysed nuclear and cytoplasmic BACH1 levels. Fig. 4D and Suppl. Fig. S4C show that in contrast with the effect
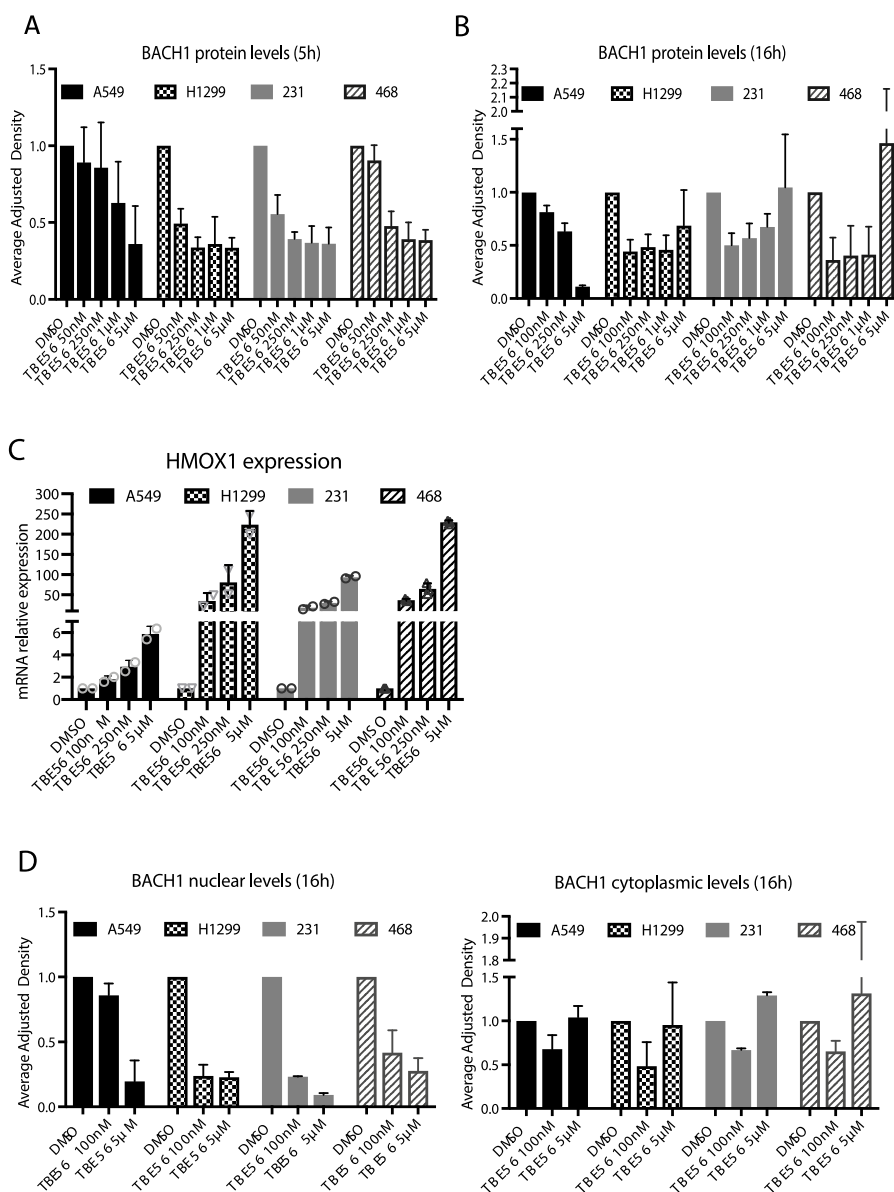
Fig. 4. TBE56 degrades BACH1 in a variety of cancer cells. A and B) A549, H1299, MDA-MB-231 (231) and MDA-MB-468 (468) cells were treated with either DMSO (0.1%, v/v) or increasing concentrations of TBE56 for 5 h (A) or 16 h (B) and the levels of BACH1 protein were analysed by Western blot. Panels show the quantification of BACH1 protein levels normalized for tubulin levels in the various cell lines. Data represent means ± SD (n = 3) and are expressed relative to each DMSO-treated sample. Representative blots are shown in Supplementary Figs. S4A and S4B. **C)** A549, H1299, MDA-MB-231 (231) and MDA-MB-468 (468) cells were treated with either DMSO (0.1%, v/v) or increasing concentrations of TBE56. After 16 h mRNA levels of *HMOX1* were analysed by real-time qPCR as previously described. *HMOX1* levels in the DMSO samples of each cell line were set to 1 and the rest of the data are expressed relative to their corresponding DMSO sample (n = 2–3). **D)** A549, H1299, MDA-MB-231 (231) or MDA-MB-468 (468) cells were treated with either DMSO (0.1%, v/v), TBE56 (100 nM) or TBE56 (5 μM). After 16 h, cells were harvested and nuclear/cytoplasmic fractions were isolated and analysed for their levels of BACH1. The figures shown are the quantifications of nuclear and cytoplasmic BACH1 levels normalised against their corresponding loading control. Data represent means ± SD (n = 3) and are expressed relative to the DMSO-treated sample in each cell line. Representative blots are shown in Supplementary Fig. S4C.

observed for total BACH1 levels, nuclear BACH1 is reduced by TBE56 in a concentration-dependent manner. However, cytoplasmic BACH1 was reduced by the low concentration of TBE56, but its levels increased in response to the high concentration of TBE56 after 16 h. This result shows that cytoplasmic BACH1 is responsible for the observed increase in total BACH1 levels and explains the absence of repression of HMOX1 with high BACH1 levels, as the cytoplasmic form of BACH1 is unable to repress HMOX1.

Although NRF2 activation can induce BACH1 transcription [12,29], NRF2 silencing did not affect the levels of nuclear or cytoplasmic BACH1 in response to TBE56 after 16 h (Suppl. Figs. S4D and S4E), showing that the effect of TBE56 on BACH1 levels is NRF2-independent.

2.4. TBE56 impairs cell migration/invasion in a BACH1-dependent manner

While NRF2 activation in cancer has tumour-promoting effects and is therefore undesirable, BACH1 inhibition/degradation has emerged as an excellent strategy to impair tumour metastasis. BACH1 is a driver of cancer cell migration and invasion, and as we have previously shown that other BACH1-targeting compounds reduce cancer cell invasion [26], we hypothesised that by degrading BACH1, TBE56 would impair cancer cell migration and invasion, while TBE31 would not. To test this hypothesis, we used the MDA-MB-231 cell line as a model, as it is highly invasive, has high levels of BACH1, and responds well to TBE56. We generated BACH1-KO MDA-MB-231 cells (Suppl. Fig. S5A) and tested the effect of both TBE31 and TBE56 on the migration and invasion of WT and BACH1-KO MDA-MB-231 cells. As shown in Fig. 5, TBE56 (but not TBE31) significantly reduced both migration (Fig. 5A) and invasion (Fig. 5B) of BACH1-proficient WT MDA-MB-231 cells to similar levels to those of BACH1-KO cells. Moreover, TBE56 did not reduce the migration or invasion of BACH1-KO MDA-MB-231 cells further (Fig. 5A and B), confirming that the anti-migration/invasion activities of TBE56 were due to its effect on BACH1.

3. Discussion

Here we found that biotinylation of the synthetic tricyclic bis(cyanoenone) TBE31 confers a novel activity against BACH1. TBE56 is a weak NRF2 activator, but a potent BACH1 degrader, with activity in both non-malignant and cancer cells. Moreover, TBE56 is over 50 times more potent than hemin in reducing the BACH1 levels, and its effect is of a longer duration. The fact that biotinylation of an electrophilic compound confers this novel activity was unexpected. We have recently reported another electrophilic NRF2 activator (CDDO) that gains BACH1-targeting properties upon modification of its polar carboxyl group (as in CDDO-Me and CDDO-TFEA) (Structures in Suppl. Fig. S5B). As electrophilicity appears to be necessary for targeting BACH1 by these compounds, we hypothesise that if the effect of these compounds is direct (as suggested by the observed interaction between TBE56 and BACH1, and by the BACH1 cysteine modification by DMF), the biotinylation could: a) facilitate the compound-BACH1 interaction by increasing its affinity, and the electrophilic moiety would then modify BACH1 leading to its degradation/nuclear export; and/or b) facilitate the degradation/nuclear export of BACH1 by promoting its interaction with a protein(s) that participates in these processes. In this context, it has been shown that adding a hydrophobic moiety on a protein surface could mimic a partially unfolded region leading to its recognition by the protein quality control machinery and its consequent chaperone-mediated proteasomal degradation [30,31]. Thus, the hydrophobic tail of the biotin group and/or the spacer arm within TBE56 could be facilitating the degradation of BACH1. It would be interesting to test whether changing the length of the spacer arm between the conjugation site in TBE31 and the biotin molecule affects its BACH1-degrading activity. This might also provide a rationale to generate novel BACH1 degraders based on known electrophilic compounds.

BACH1-targeting compounds and NRF2 activators that act by inhibiting KEAP1 share a similar therapeutic potential for chronic conditions. However, BACH1-targeting compounds have the advantage of also being promising drugs in cancer due to their anti-metastatic potential. While for chronic conditions compounds targeting both KEAP1 and BACH1 might be excellent drugs, a compound targeting just BACH1 might be preferable in a cancer setting. Here we show that low concentrations of TBE56 impair the migration and invasion of triple negative breast cancer cells in a BACH1-dependent manner, providing a rationale for a further optimisation and testing of this (or similar) compounds in pre-clinical models of breast cancer metastasis. Although TBE31 has been tested *in vivo* showing good pharmacokinetic (PK) and pharmacodynamic (PD) properties with excellent bioavailability following oral administration [32], TBE56 has not been tested *in vivo*, and thus its translational potential is still unknown. Nonetheless, our work provides a rationale for the design of new TBE31 derivatives with BACH1-targetting activities while maintaining its PK and PD properties.

4. Material and methods

4.1. Cell culture

Cells were grown in RPMI (HaCaT) or DMEM (H1299, A549, MDA-MB-231 and MDA-MB-468) containing 10% FBS at 37 °C and 5% CO2. HaCaT cells have been validated by STR profiling. H1299, A549, MDA-MB-231 and MDA-MB-468 cells were obtained from ATCC. All cells were
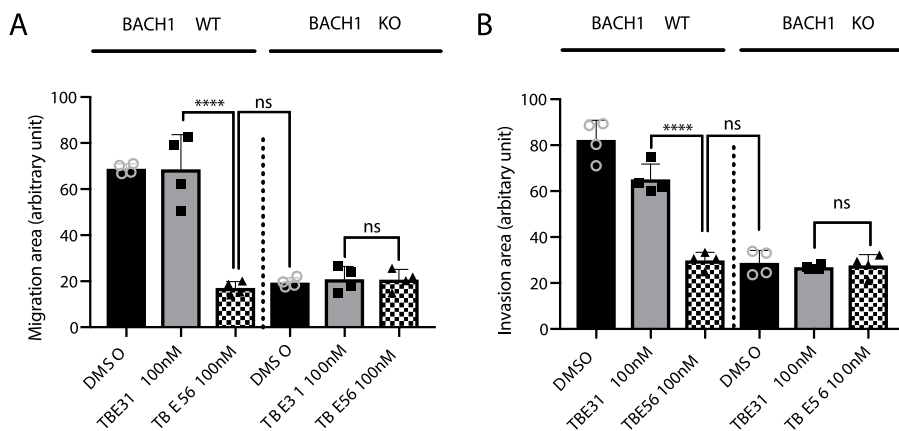
Fig. 5. TBE56 impairs cell migration and invasion in a BACH1-dependent manner. A) MDA-MB-231 WT and BACH1-KO cells were treated with DMSO (0.1%, v/v), TBE31 (100 nM) or TBE56 for 6 h, followed by transwell migration (without Matrigel) and invasion (with Matrigel) assays (n = 4).

routinely tested for mycoplasma. CRISPR-edited NRF2-KO and BACH1-KO cells were produced as previously described [26,33]. Control cells, referred to wild type (WT) are the pooled population of surviving cells transfected with an empty pLentiCRISPRv2 vector treated with the appropriate antibiotic (puromycin or blasticidin). In short: The endogenous *BACH1* or *NFE2L2* gene, were edited by transfecting cells with pLentiCRISPR-v2 (a gift from Dr Feng Zhang, Addgene plasmid #52961) containing single-guide (sg) RNAs directed against *BACH1* (CGATGT-CACCATCTTTGTGG and GACTCTGAGACGGACACCGA) or the KEAP1-binding domain within the *NFE2L2* locus (TGGAGGCAAGATA-TAGATCT). For the generation of MDA-MB-231 BACH1-KO cells a sgRNA targeting human *BACH1 (*CCACTCAAGAATCGTAGGCC) was expressed in the pLentiCRISPRv2-blast (#98293, Addgene).

4.2. Antibodies and reagents

Antibodies against Beta-ACTIN (C-4), BACH1 (F-9) and LAMIN B2 (C-20) were obtained from Santa Cruz Biotechnology (Dallas, Texas, USA). *Anti*-FBX022 antibody (13606-1-AP) was obtained from Proteintech (Manchester, UK). *Anti*-NRF2 antibody (D1Z9C) was obtained from Cell Signalling Technology (Danvers, MA, USA) and *anti*-HMOX1 antibody was purchased from Biovision (San Francisco, CA, USA). Antibody against ALPHA-TUBULIN was obtained from Sigma-Aldrich (St. Louis, MO, USA). HRP-conjugated secondary antibodies were obtained from Life Technologies (Carlsbad, California, USA). Dimethyl sulfoxide (DMSO) was from Sigma-Aldrich. CDDO-Me was obtained from Cayman Chemicals (Ann Arbor, MI, USA). MG132 was obtained from Santa Cruz Biotechnology. MLN4924 was obtained from Selleckchem (Houston, TX, USA). (±)-TBE31, and biotinylated TBE31 (TBE56) were synthesized as described [27,34,35]. MG132 was obtained from Santa Cruz Biotechnology.

4.3. siRNA transfections

On the day prior to transfection, cells were plated to the required cell density (70–90% confluency). The siRNA and Lipofectamine RNAiMAX (Invitrogen, Carlsbad, CA, USA) were individually diluted in Optimem (Life Technologies) and incubated for 10 min at room temperature. Diluted siRNA was added to the diluted Lipofectamine solution (1:1 ratio) and further incubated for 15 min. The complex was added to the cells and incubated in a humidified incubator at 37 °C and 5% CO_2 for 36 h prior to treatment and lysis. All siRNAs used were OnTargetplus SMARTPool siRNAs (mixture of 4 siRNAs provided as a single reagent) obtained from Horizon Discovery.

4.4. Plasmids

BACH1-RFP, and BACH1- Hemin resistant (4CA) -RFP (containing C435A, C46A, C492A and C646A) were generated by cloning the synthesised inserts into Plenti-CMV-MCS-RFP-SV-puro (a gift from Jonathan Garlick & Behzad Gerami-Naini. Addgene plasmid # 109377).

4.5. Quantitative real time PCR (rt-qPCR)

RNA from cells was extracted using GeneJET RNA Purification Kit (Thermo Fisher Scientific) and 500 ng of RNA per sample was reverse-transcribed to cDNA using Omniscript RT kit (Qiagen) supplemented with RNase inhibitor according to the manufacturer's instructions. Resulting cDNA was analysed using TaqMan Universal Master Mix II (Life Technologies, Carlsbad, CA, USA) as well as corresponding Taqman probes. Gene expression was determined using a QuantStudio 7 Flex qPCR machine by the comparative ΔΔCT method. All experiments were performed at least in triplicates and data were normalized to the housekeeping gene HPRT1. Taqman probes used: HPRT1 Hs02800695_m1; HMOX1 Hs01110250_m1; AKR1B10 Hs00252524_m1; BACH1 Hs00230917_m1.

4.6. Cell lysis and Western blot

Cells were washed and harvested in ice-cold phosphate-buffered saline (PBS). For whole-cell extracts, cells were lysed in RIPA buffer supplemented with phosphatase and protease inhibitors. Lysates were sonicated for 15 s at 20% amplitude and then cleared by centrifugation for 15 min at 4 °C. For subcellular fractionation, cells were resuspended in 400 μl of low-salt buffer A (10 mM Hepes/KOH pH7.9, 10 mM KCL, 0.1 mM EDTA, 0.1 mM EGTA, 1 mM β-mercaptoethanol) and after incubation for 10 min on ice, 10 μl of 10% NP-40 was added and cells were lysed by gently vortexing. The homogenate was centrifuged for 10 s at 13,200 rpm, the supernatant representing the cytoplasmic fraction was collected and the pellet containing the cell nuclei was washed 4 additional times in buffer A. The pellet containing the nuclear fraction was then resuspended in 100 μl high-salt buffer B (20 mM Hepes/KOH pH7.9, 400 mM NaCl, 1 mM EDTA, 1 mM EGTA, 1 mM β-mercaptoethanol). The lysates were sonicated and centrifuged at 4 °C for 15 min at 13,200 rpm. The supernatant representing the nuclear fraction was collected. Protein concentration was determined using the BCA assay (Thermo Fisher Scientific, Waltham, MA, USA). Lysates were mixed with SDS sample buffer and boiled for 7 min at 95 °C. Equal amounts of protein were separated by SDS-PAGE, followed by semidry blotting to a polyvinylidene difluoride membrane (Thermo Fisher Scientific). After blocking of the membrane with 5% (w/v) non-fat dried milk dissolved in Tris buffered saline (TBS) with 0.1% v/v Tween-20 (TBST), membranes were incubated with the primary antibodies overnight at 4 °C. Appropriate secondary antibodies coupled to horseradish peroxidase were detected by enhanced chemiluminescence using ClarityTM Western ECL Blotting Substrate (Bio-Rad, Hercules, CA, USA). Resulting protein bands were quantified and normalised to each lane's loading control using the ImageStudio Lite software (LI-COR). For whole cell extracts, the protein of interest was normalised against ACTIN or TUBULIN. LAMIN was used as an internal control for nuclear extracts and TUBULIN was used as controls for cytoplasmic extracts.

4.7. Pull down assay

Cells were washed and harvested in ice-cold phosphate-buffered saline (PBS) and lysed in IP buffer (50 mM Hepes pH 7.5, 50 mM NaCl, 1% (v/v) Triton X-100, 2 mM EDTA, 10 mM sodium fluoride, 0.5 mM sodium orthovanadate, leupeptine (10 μg/ml), aprotinin (10 μg/ml). Lysates were sonicated for 15 s at 20% amplitude and then cleared by centrifugation for 15 min at 4 °C. 10% of the total volume was used as an INPUT material. The pull-down was performed with 20 μl of Dynabeads™ M − 270 Streptavidin. Tubes were rotated for 30 min on a spinning wheel at 4 °C. The beads were washed 3x with IP buffer and eluted by boiling in 1 x SDS sample buffer.

4.8. Cell viability assay

Alamar Blue (Thermo Fisher Scientific) was used to determine cell viability after drug treatment. Cells were seeded in 96-well plates to 50–60% confluency and treated on the next day with the corresponding compounds for 48 h. After treatment, Alamar Blue was added to the wells (1:10 ratio) and after 4 h of incubation at 37 °C, the fluorescence was measured (excitation 550 nm/emission 590 nm) using a microplate reader (Spectramax M2). Viability was calculated relative to DMSO-treated control cells.

4.9. Cell migration and invasion assays

Transwell migration and invasion assays were performed with 6.5-mm inserts with 8.0-μm-pore membrane. Cells were treated for 6 h with the corresponding compounds, and then cells (6×10^4/well) were resuspended in serum-free medium in the upper chamber with the corresponding compounds. The bottom chamber contained complete

medium with 10% FBS supplemented with the corresponding compounds to avoid any drug gradient. For invasion assays, the inserts were precoated with a 1:30 dilution of Matrigel (Corning 356234). After 15 h, cells in the upper chamber were removed with a humidified cotton swab, and invading cells on the other side of the membrane were fixed with PFA, stained with crystal violet, and photographed under a bright-field microscope (5X). The area covered by cells on each field of views was quantified with ImageJ on at least five fields per well.

Statistical analysis

Experiments were repeated at least 2–7 times with multiple technical replicates to be eligible for the indicated statistical analyses. Data were analysed using Graphpad Prism statistical package. All results are presented as mean ± SD unless otherwise mentioned. The differences between groups were analysed using two-way ANOVA.

Authors contribution

RM, LC, MH, and KXA conducted the experiments and were responsible for initial data analysis, figure preparation and statistical analysis. TH, CW and VIS provided resources and technical expertise. LV had a leading contribution in the design of the study, and ADK an active role in the discussion and interpretation of the whole dataset. LV wrote the original draft of the manuscript. All authors reviewed and edited the manuscript. Funding acquisition LV, ADK VIS and CW. All authors take full responsibility for the work.

Data availability

No data was used for the research described in the article.

Appendix A. Supplementary data

Supplementary data to this article can be found online at https://doi.org/10.1016/j.freeradbiomed.2022.08.041.

References

[1] L. Casares, J.D. Unciti-Broceta, M.E. Prados, D. Caprioglio, D. Mattoteia, M. Higgins, et al., Isomeric O-methyl cannabidiolquinones with dual BACH1/NRF2 activity, Redox Biol. 37 (2020), 101689.
[2] M. Ahuja, N. Ammal Kaidery, O.C. Attucks, E. McDade, D.M. Hushpulian, A. Gaisin, et al., Bach1 derepression is neuroprotective in a mouse model of Parkinson's disease, Proc. Natl. Acad. Sci. U. S. A. 118 (45) (2021).
[3] S. Wada, H. Kanzaki, Y. Katsumata, Y. Yamaguchi, T. Narimiya, O.C. Attucks, et al., Bach1 inhibition suppresses osteoclastogenesis via reduction of the signaling via reactive oxygen species by reinforced antioxidation, Front. Cell Dev. Biol. 8 (2020) 740.
[4] M. Inoue, S. Tazuma, K. Kanno, H. Hyogo, K. Igarashi, K. Chayama, Bach1 gene ablation reduces steatohepatitis in mouse MCD diet model, J. Clin. Biochem. Nutr. 48 (2) (2011) 161–166.
[5] Y. Watari, Y. Yamamoto, A. Brydun, T. Ishida, S. Mito, M. Yoshizumi, et al., Ablation of the bach1 gene leads to the suppression of atherosclerosis in bach1 and apolipoprotein E double knockout mice, Hypertens. Res. 31 (4) (2008) 783–792.
[6] K. Kondo, Y. Ishigaki, J. Gao, T. Yamada, J. Imai, S. Sawada, et al., Bach1 deficiency protects pancreatic beta-cells from oxidative stress injury, Am. J. Physiol. Endocrinol. Metab. 305 (5) (2013) E641–E648.
[7] M. von Scheidt, Y. Zhao, T.Q. de Aguiar Vallim, N. Che, M. Wierer, M.M. Seldin, et al., Transcription factor MAFF (MAF basic leucine zipper transcription factor F)

[8] regulates an atherosclerosis relevant network connecting inflammation and cholesterol metabolism, Circulation 143 (18) (2021) 1809–1823.
[8] H. Zhang, L. Zhou, K.J.A. Davies, H.J. Forman, Silencing Bach1 alters aging-related changes in the expression of Nrf2-regulated genes in primary human bronchial epithelial cells, Arch. Biochem. Biophys. 672 (2019), 108074.
[9] J.F. Reichard, G.T. Motz, A. Puga, Heme oxygenase-1 induction by NRF2 requires inactivation of the transcriptional repressor BACH1, Nucleic Acids Res. 35 (21) (2007) 7074–7086.
[10] J. Sun, H. Hoshino, K. Takaku, O. Nakajima, A. Muto, H. Suzuki, et al., Hemoprotein Bach1 regulates enhancer availability of heme oxygenase-1 gene, EMBO J. 21 (19) (2002) 5216–5224.
[11] M. Sato, M. Matsumoto, Y. Saiki, M. Alam, H. Nishizawa, M. Rokugo, et al., BACH1 promotes pancreatic cancer metastasis by repressing epithelial genes and enhancing epithelial-mesenchymal transition, Cancer Res. 80 (6) (2020) 1279–1292.
[12] L. Lignitto, S.E. LeBoeuf, H. Homer, S. Jiang, M. Askenazi, T.R. Karakousi, et al., Nrf2 activation promotes lung cancer metastasis by inhibiting the degradation of Bach1, Cell 178 (2) (2019) 316–29 e18.
[13] J. Lee, A.E. Yesilkanal, J.P. Wynne, C. Frankenberger, J. Liu, J. Yan, et al., Effective breast cancer combination therapy targeting BACH1 and mitochondrial metabolism, Nature 568 (7751) (2019) 254–258.
[14] H.J. Warnatz, D. Schmidt, T. Manke, I. Piccini, M. Sultan, T. Borodina, et al., The BTB and CNC homology 1 (BACH1) target genes are involved in the oxidative stress response and in control of the cell cycle, J. Biol. Chem. 286 (26) (2011) 23521–23532.
[15] A.K. MacLeod, M. McMahon, S.M. Plummer, L.G. Higgins, T.M. Penning, K. Igarashi, et al., Characterization of the cancer chemopreventive NRF2-dependent gene battery in human keratinocytes: demonstration that the KEAP1-NRF2 pathway, and not the BACH1-NRF2 pathway, controls cytoprotection against electrophiles as well as redox-cycling compounds, Carcinogenesis 30 (9) (2009) 1571–1580.
[16] C. Wiel, K. Le Gal, M.X. Ibrahim, C.A. Jahangir, M. Kashif, H. Yao, et al., BACH1 stabilization by antioxidants stimulates lung cancer metastasis, Cell 178 (2) (2019) 330–45 e22.
[17] Y. Liang, H. Wu, R. Lei, R.A. Chong, Y. Wei, X. Lu, et al., Transcriptional network analysis identifies BACH1 as a master regulator of breast cancer bone metastasis, J. Biol. Chem. 287 (40) (2012) 33533–33544.
[18] W. Han, Y. Zhang, C. Niu, J. Guo, J. Li, X. Wei, et al., BTB and CNC homology 1 (Bach1) promotes human ovarian cancer cell metastasis by HMGA2-mediated epithelial-mesenchymal transition, Cancer Lett. 445 (2019) 45–56.
[19] N. Shajari, S. Davudian, T. Kazemi, B. Mansoori, S. Salehi, V. Khaze Shahgoli, et al., Silencing of BACH1 inhibits invasion and migration of prostate cancer cells by altering metastasis-related gene expression, Artif. Cell Nanomed. Biotechnol. 46 (7) (2018) 1495–1504.
[20] S. Davudian, N. Shajari, T. Kazemi, B. Mansoori, S. Salehi, A. Mohammadi, et al., BACH1 silencing by siRNA inhibits migration of HT-29 colon cancer cells through reduction of metastasis-related genes, Biomed. Pharmacother. 84 (2016) 191–198.
[21] L. Casares, V. Garcia, M. Garrido-Rodriguez, E. Millan, J.A. Collado, A. Garcia-Martin, et al., Cannabidiol induces antioxidant pathways in keratinocytes by targeting BACH1, Redox Biol. 28 (2020), 101321.
[22] O.C. Attucks, K.J. Jasmer, M. Hannink, J. Kassis, Z. Zhong, S. Gupta, et al., Induction of heme oxygenase I (HMOX1) by HPP-4382: a novel modulator of Bach1 activity, PLoS One 9 (7) (2014), e101044.
[23] K. Ogawa, J. Sun, S. Taketani, O. Nakajima, C. Nishitani, S. Sassa, et al., Heme mediates derepression of Maf recognition element through direct binding to transcription repressor Bach1, EMBO J. 20 (11) (2001) 2835–2843.
[24] J.W. Kaspar, A.K. Jaiswal, Antioxidant-induced phosphorylation of tyrosine 486 leads to rapid nuclear export of Bach1 that allows Nrf2 to bind to the antioxidant response element and activate defensive gene expression, J. Biol. Chem. 285 (1) (2010) 153–162.
[25] H. Suzuki, S. Tashiro, S. Hira, J. Sun, C. Yamazaki, Y. Zenke, et al., Heme regulates gene expression by triggering Crm1-dependent nuclear export of Bach1, EMBO J. 23 (13) (2004) 2544–2553.
[26] L. Casares, R. Moreno, K.X. Ali, M. Higgins, S. Dayalan Naidu, G. Neill, et al., The synthetic triterpenoids CDDO-TFEA and CDDO-Me, but not CDDO, promote nuclear exclusion of BACH1 impairing its activity, Redox Biol. 51 (2022), 102291.
[27] A. Saito, M. Higgins, S. Zheng, W. Li, I. Ojima, A.T. Dinkova-Kostova, et al., Synthesis and biological evaluation of biotin conjugates of (+/-)-(4bS,8aR,10aS)-10a-ethynyl-4b,8,8-trimethyl-3,7-dioxo-3,4b,7,8,8a,9,10,10a- octahydro-phenanthrene-2,6-dicarbonitrile, an activator of the Keap1/Nrf2/ARE pathway, for the isolation of its protein targets, Bioorg. Med. Chem. Lett 23 (20) (2013) 5540–5543.
[28] Y. Zenke-Kawasaki, Y. Dohi, Y. Katoh, T. Ikura, M. Ikura, T. Asahara, et al., Heme induces ubiquitination and degradation of the transcription factor Bach1, Mol. Cell Biol. 27 (19) (2007) 6962–6971.
[29] H.K. Jyrkkanen, S. Kuosmanen, M. Heinaniemi, H. Laitinen, E. Kansanen, E. Mella-Aho, et al., Novel insights into the regulation of antioxidant-response-element-mediated gene expression by electrophiles: induction of the transcriptional repressor BACH1 by Nrf2, Biochem. J. 440 (2) (2011) 167–174.
[30] S.R. Choi, H.M. Wang, M.H. Shin, H.S. Lim, Hydrophobic tagging-mediated degradation of transcription coactivator SRC-1, Int. J. Mol. Sci. 22 (12) (2021).
[31] P.M. Cromm, C.M. Crews, Targeted protein degradation: from chemical biology to drug Discovery, Cell Chem. Biol. 24 (9) (2017) 1181–1190.
[32] R.V. Kostov, E.V. Knatko, L.A. McLaughlin, C.J. Henderson, S. Zheng, J.T. Huang, et al., Pharmacokinetics and pharmacodynamics of orally administered acetylenic

tricyclic bis(cyanoenone), a highly potent Nrf2 activator with a reversible covalent mode of action, Biochem. Biophys. Res. Commun. 465 (3) (2015) 402–407.

[33] L. Torrente, C. Sanchez, R. Moreno, S. Chowdhry, P. Cabello, K. Isono, et al., Crosstalk between NRF2 and HIPK2 shapes cytoprotective responses, Oncogene 36 (44) (2017) 6204–6212.

[34] A. Saito, S.Q. Zheng, M. Takahashi, W. Li, I. Ojima, T. Honda, An improved synthesis of a hydroxymethyl tricyclic ketone from cyclohexanone, the key

processes for the synthesis of a highly potent anti-inflammatory and cytoprotective agent, Synthesis-Stuttgart 45 (23) (2013) 3251–3254.

[35] T. Honda, H. Yoshizawa, C. Sundararajan, E. David, M.J. Lajoie, F.G. Favaloro Jr., et al., Tricyclic compounds containing nonenolizable cyano enones. A novel class of highly potent anti-inflammatory and cytoprotective agents, J. Med. Chem. 54 (6) (2011) 1762–1778.